Feedback regulation of p38 activity via ATF2 is essential for survival of embryonic liver cells

Wolfgang Breitwieser,[1] Steve Lyons,[1] Ann Marie Flenniken,[1,5] Garry Ashton,[2] Gail Bruder,[1] Mark Willington,[1] Georges Lacaud,[3] Valerie Kouskoff,[4] and Nic Jones[1,6]

[1]Cell Regulation Department, Paterson Institute for Cancer Research, University of Manchester, Manchester M20 4BX, United Kingdom; [2]Histology Department, Paterson Institute for Cancer Research, University of Manchester, Manchester M20 4BX, United Kingdom; [3]Stem Cell Biology Department, Paterson Institute for Cancer Research, University of Manchester, Manchester M20 4BX, United Kingdom; [4]Stem Cell and Haematopoiesis Department, Paterson Institute for Cancer Research, University of Manchester, Manchester M20 4BX, United Kingdom

The ATF2 transcription factor is phosphorylated by the stress-activated mitogen-activated protein kinases (MAPKs) JNK and p38. We show that this phosphorylation is essential for ATF2 function in vivo, since a mouse carrying mutations in the critical phosphorylation sites has a strong phenotype identical to that seen upon deletion of the DNA-binding domain. In addition, combining this mutant with a knockout of the ATF2 homolog, ATF7, results in embryonic lethality with severe abnormalities in the developing liver and heart. The mutant fetal liver is characterized by high levels of apoptosis in developing hepatocytes and haematopoietic cells. Furthermore, we observe a significant increase in active p38 due to loss of a negative feedback loop involving the ATF2-dependent transcriptional activation of MAPK phosphatases. In embryonic liver cells, this increase drives apoptosis, since it can be suppressed by chemical inhibition of p38. Our findings demonstrate the importance of finely regulating the activities of MAPKs during development.

[*Keywords*: ATF2; AP-1; p38; MAPK; DUSP1; apoptosis]

Supplemental material is available at http://www.genesdev.org.

Received February 22, 2007; revised version accepted June 28, 2007.

The AP-1 transcription factor consists of a number of structurally related proteins including the Jun, Fos, and ATF family of bZip proteins. Binding to transcriptional target sequences occurs via dimerization, and various combinations of AP-1 dimerization partners can achieve a great amount of functional diversity among AP-1 members (Eferl and Wagner 2003). The ATF2 family consists of three members, ATF2, ATF7 (ATFa), and CREBPa (Vinson et al. 2002). While ATF2 forms homodimers that bind CRE-like recognition sequences, the heterodimers with other AP-1 family members such as cJun allow it to bind typical AP-1 sequences (Benbrook and Jones 1990; Ivashkiv et al. 1990; Hai and Curran 1991). This ability provides ATF2 with huge versatility with regard to its transcriptional activity and is a feature that is reflected in the multitude of reported ATF2 target genes and transcriptional functions. Diversity in AP-1 activity is also generated through its regulation by upstream kinases. For example, cJun contains an N-terminal transcription-activation domain that is regulated by mitogen-activated protein kinases (MAPKs) ERK and JNK (Pulverer et al. 1991; Smeal et al. 1991; Derijard et al. 1994). Mouse knock-in experiments have shown that while deletion of cJun itself is embryonic lethal, the two JNK-specific phosphorylation sites in its N-terminal activation domain (Ser63 and Ser73) are dispensable for embryonic development (Behrens et al. 1999). Nonetheless, phosphorylation of these sites is essential for induction of stress or tumor necrosis factor α-induced apoptosis (Behrens et al. 1999, 2001).

ATF2 also contains an N-terminal activation domain (Livingstone et al. 1995; van Dam et al. 1995) that, like cJun, is activated by ERK, JNK, and, in addition, by stress and cytokine-activated MAPK p38 (Derijard et al. 1994; Kyriakis et al. 1994; Gupta et al. 1995; Raingeaud et al. 1995; Ouwens et al. 2002). Therefore, ATF2 is responsive to a host of environmental and cellular stimuli ranging from mitogenic signals via the regulation through ERK or stress signals via regulation through JNK and p38. Mouse knockouts have shown that ATF2 is essential in animal development (Reimold et al. 1996; Maekawa et al. 1999) and has an important role in stress response

[5]Present address: Centre for Modeling Human Disease, Samuel Lunenfeld Research Institute, Mount Sinai Hospital, 600 University Avenue, Toronto, Ontario M5G 1X5, Canada.
[6]Corresponding author.
E-MAIL njones@picr.man.ac.uk; FAX 44-161-4463038.
Article is online at http://www.genesdev.org/cgi/doi/10.1101/gad.430207.

(Reimold et al. 2001). MAPK-dependent phosphorylation of ATF2 occurs at Thr69, Thr71, and Ser91, and at least Thr69 and Thr71 are necessary for the ability of ATF2 to activate transcription in response to UV and genotoxic agents in cultured cells (Gupta et al. 1995; Livingstone et al. 1995; van Dam et al. 1995). However, while phosphorylated ATF2 is commonly used as an indicator of increased JNK or p38 activity in human or animal tissues, the in vivo role of ATF2 N-terminal phosphorylation remains unresolved. To address this question, we generated a mouse knock-in in which phosphor acceptor residues corresponding to Thr69 and Thr71 of human ATF2 were mutated to alanines. This mutated ATF2 protein still binds DNA on target promoters, but it is no longer functional, as the knock-in leads to the same onset and rate of mortality that is seen with a deletion of its DNA-binding domain. In addition, we show that a knockout of the closest ATF2 homolog, ATF7, in combination with the ATF2 phosphorylation mutant or the deletion mutant in the DNA-binding domain, produces a complexity of defects involving the developing heart and liver that lead to embryonic lethality. In the embryonic liver, ATF2/7 activation and functions are required for initiating anti-apoptotic mechanisms and are likely effectors of signaling by MKK4, a MAPK kinase-activating JNK and p38 activities, based on the very similar phenotypes that are seen in both MKK4 and ATF2/7 mutant embryos. We further show that ATF2/7 are required to limit p38 kinase activity through a negative feedback involving the transcriptional activation of MAPK phosphatases, thus providing an underlying mechanism for the anti-apoptotic functions of ATF2/7 in the developing liver.

Results

ATF2 N-terminal phosphorylation is essential

In reporter assays the phosphorylation of Thr69 and Thr71 is essential for the transcriptional activity of ATF2, and this phosphorylation correlates with cellular responses to many external stimuli and stresses (Gupta et al. 1995; Livingstone et al. 1995; van Dam et al. 1995). To test the in vivo significance of the N-terminal phosphorylation of ATF2 we mutated the two sites in mouse ATF2 (Fig. 1A). Thus, the genomic sequence in exon 4 of the mouse ATF2 was altered such that Thr51 and Thr53, which correspond to human ATF2 Thr69 and Thr71, respectively, were mutated into alanines ($ATF2^{AA}$) and a knock-in mouse was produced.

To verify that the point mutations were maintained in the germline, mouse embryonic fibroblasts (MEFs) were produced from embryos that were the result of crosses between heterozygote ($Atf2^{AA/+}$) mice, and the sequence of the genomic region containing the mutated codons was determined (Fig. 1B). Furthermore, MEFs derived

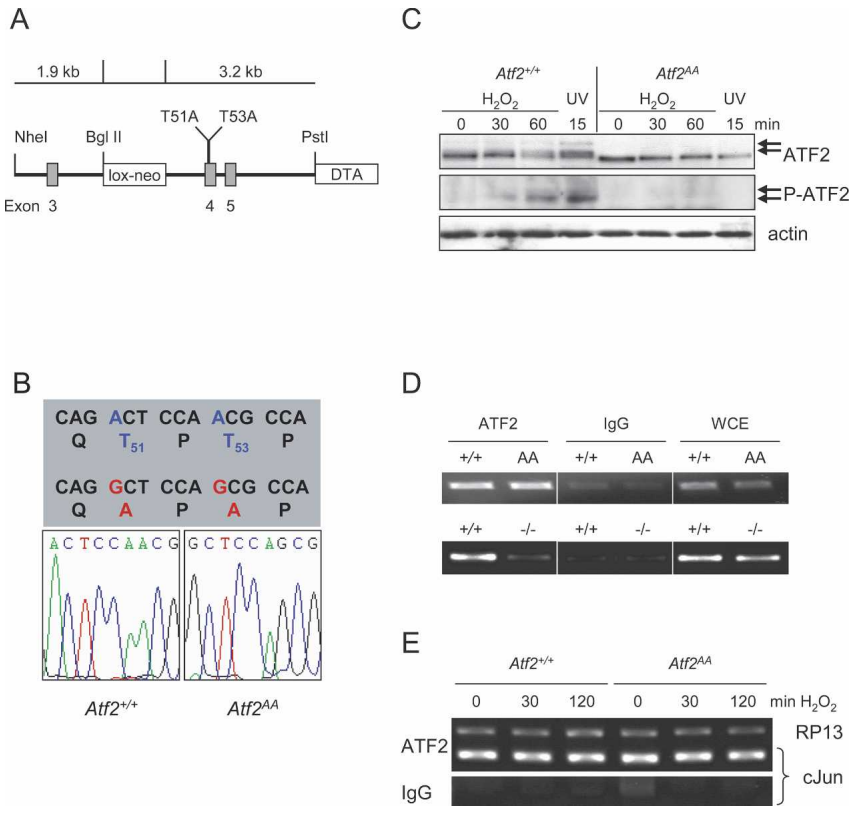

Figure 1. Generation of ATF2 N-terminal phosphorylation mutant mice. (*A*) A schematic representation of the $Atf2^{AA}$ knock-in strategy. Positions of exons 3–5 are shown (gray boxes). An excisable neomycin resistance gene (*lox-neo*) is inserted into intron 3 and a negative selection marker (*Diphtheria toxin A*, *DTA*) is inserted into intron 5 and flanks the linearized targeting vector. (*B*) Sequence of wild-type and $Atf2^{AA}$ gene in MEFs from homozygous knock-in animals encompassing the point mutations (red) leading to threonine-to-alanine substitutions at positions 51 and 53 of mouse ATF2. (*C*) Western blot analysis of wild-type and $Atf2^{AA}$ MEFs after oxidative stress (100 µM H_2O_2) or radiation (80 J/m^2 UV). Absence of phosphorylated ATF2 bands (arrows) is apparent in $Atf2^{AA}$ extracts using antibodies recognizing pan-ATF2 and phospho-T53 (P-ATF2). β-actin is shown as loading control. (*D*) PCR analysis of *cJun* promoter containing the ATF-binding site *jun2* from $Atf2^{+/+}$ versus $Atf2^{AA}$ (*top* panel) and $Atf2^{+/+}$ versus $Atf2^{-/-}$ (*bottom* panel) MEFs immunoprecipitated with ATF2 antibodies or control antibodies (IgG). Whole-cell extracts (WCE) were used as PCR controls. (*E*) ChIP analysis using ATF2 antibodies of *cJun* promoter versus unregulated *RP13* promoter before and after stress induction by H_2O_2 (100 µM). (*Bottom* panel) No significant binding to the *cJun* promoter is detected with IgG control.

from wild-type ($Atf2^{+/+}$) and homozygous mutant ($Atf2^{AA}$) embryos were stressed to induce JNK and p38 kinase activity and protein extracts were probed with ATF2-specific antibodies (Fig. 1C). After stress induction, extracts from wild-type cells revealed slower migrating bands of ATF2 corresponding to phosphorylated forms. In contrast, while $Atf2^{AA}$ extracts contained levels of ATF2 protein comparable with wild type, no migratory shift of ATF2 protein was apparent after stress induction. In addition, while phospho-specific ATF2 antibodies recognized phospho-Thr53 in wild-type extracts, no phospho-specific signal was apparent in $Atf2^{AA}$, confirming the lack of significant N-terminal phosphorylation (Fig. 1C). Chromatin immunoprecipitation (ChIP) was used to compare binding abilities of $ATF2^{+/+}$, $ATF2^{AA}$, and $ATF2^{-/-}$, a mutant form of ATF2 that contains a deletion in the DNA-binding domain (Supplementary Fig. S1), and therefore is similar to the previously reported $ATF2^{0/0}$ (Maekawa et al. 1999). In ChIPs, $ATF2^{+/+}$ and $ATF2^{AA}$ bind comparatively to ATF-binding sites in the *cJun* gene (Fig. 1D), as well as in *Atf3* or *Cyclin D1* genes (data not shown). As would be expected, $ATF2^{-/-}$ fails to bind *cJun* promoter sequences (Fig. 1D). In addition, the presence of ATF2 on the *cJun* promoter does not alter depending on its activation, as binding of $ATF2^{+/+}$ and $ATF2^{AA}$ is comparable before and after stimulating conditions (Fig. 1E).

To test the consequences of the N-terminal mutations, we crossed heterozygote animals and determined the genotypes of the offspring. Strikingly, no $Atf2^{AA}$ adult mice were found, suggesting that $Atf2^{AA}$ is lethal (Table 1). However, among the offspring from heterozygote crosses that were delivered by ceasarian section at day 18 post-coitum, we found approximately the expected number of embryos homozygous for $Atf2^{AA}$, all of which were alive at the time of delivery and comparable with their littermates in physical appearance and weight (data not shown). Thus, no significant loss of $Atf2^{AA}$ embryos occurred during embryonic development. However, all $Atf2^{AA}$ animals that were born naturally died within the first few hours after birth. Examination of newborn mice revealed that the $Atf2^{AA}$ animals were cyanotic in appearance, reminiscent of the phenotype of the previously reported $Atf2^{0/0}$ mutants (Maekawa et al. 1999). Similarly, this phenotype was also observed in $Atf2^{-/-}$ (data not shown). Therefore, the $Atf2^{AA}$ allele, resulting in a similar phenotype to that caused by deletions in the DNA-binding domain, reveals that N-terminal phosphorylation is essential for ATF2 function and vital for animal survival.

Table 1. *Offspring genotypes from* $Atf2^{AA/+} \times Atf2^{AA/+}$ *and* $Atf7^{+/-} \times Atf7^{+/-}$ *crosses*

	Number of offspring		
	E18.5	Newborn	Adult
$Atf2^{AA/+} \times Atf2^{AA/+}$			
$Atf2^{+/+}$	19 (21.3%)	23 (26.4%)	13 (36.1%)
$Atf2^{AA/+}$	52 (58.4%)	48 (55.2%)	23 (63.9%)
$Atf2^{AA}$	18 (20.2%)	16[a] (18.4%)	0 (0%)
Total number	89 ($P > 0.05$)	87 ($P > 0.05$)	36 ($P < 0.01$)
$Atf7^{+/-} \times Atf7^{+/-}$			
$Atf7^{+/+}$	n.d.	n.d.	56 (25.2%)
$Atf7^{+/-}$	n.d.	n.d.	118 (53.2%)
$Atf7^{-/-}$	n.d.	n.d.	48 (21.6%)
Total number			222 ($P > 0.05$)

[a]All die within hours after birth (some loss of pups is likely to have occurred due to maternal cannibalism).
Offspring genotypes from $Atf7^{AA/+} \times Atf2^{AA/+}$ crosses were determined at E18.5, and in newborn and adult animals. Genotypes from $Atf7^{+/-} \times Atf7^{+/-}$ crosses were determined at the adult stage only. Percentages with respect to total offspring numbers are shown in brackets. Significance of distribution was calculated using χ^2 test.

$Atf2^{AA}/Atf7^{-/-}$ *causes embryonic lethality*

ATF2 shares considerable sequence homology with another ATF family member, ATF7 (also known as ATFa), especially in the N-terminal activation domain and the DNA-binding/dimerization domain, in which both proteins are almost identical. Like ATF2, ATF7 dimerizes with other AP-1 partners and is regulated via JNK and p38 (Chatton et al. 1994; Bocco et al. 1996). In addition, ATF7 is expressed in a number of adult and embryonic tissues that also express ATF2 (W. Breitwieser and N. Jones, unpubl.). We therefore considered whether ATF2 and ATF7 share overlapping functions in mouse development and whether, in the absence of either or both functional proteins, new deficiencies would emerge. $Atf7^{-/-}$ mice were produced as a result of deleting the DNA-binding and dimerization domain of ATF7 (Supplementary Fig. S2). Homozygous offspring derived from crosses between $Atf7^{+/-}$ mice are viable and no severe abnormalities were observed in adult animals (Table 1). Further crosses of $Atf7^{-/-}$ mice with $Atf2^{AA/+}$ mice resulted in $Atf2^{AA/+}/Atf7^{-/-}$ mice, which were maintained as a line that was viable and which was used to produce double homozygous offspring. Significantly, from these crosses, no ATF2/7 double homozygous mutant offspring emerged at birth. Analysis of embryos revealed that while between embryonic days 11.5 and 12.5 (E11.5 and E12.5) $Atf2^{AA}/Atf7^{-/-}$ embryos were found close to the expected numbers (Supplementary Fig. S3), many double mutant embryos displayed severe abnormalities, including developmental arrest and death (Fig. 2B). In a comparison between different mutant combinations we found that the defects in $Atf2^{AA}/Atf7^{-/-}$ embryos arose at least as early as in $Atf2^{-/-}/Atf7^{-/-}$ embryos (Fig. 2A). Therefore, in the absence of functional ATF7, the loss of N-terminal phosphorylation in ATF2 has a similar deleterious effect on embryonic development as the loss in dimerization and DNA-binding ability.

Severe heart and liver defects in ATF2/7 mutant embryos

The developmental defects in $Atf2^{AA}/Atf7^{-/-}$ and $Atf2^{-/-}/Atf7^{-/-}$ embryos ranged from anemia to severe growth retardation and arrest (Fig. 2B) with the rate of severity of

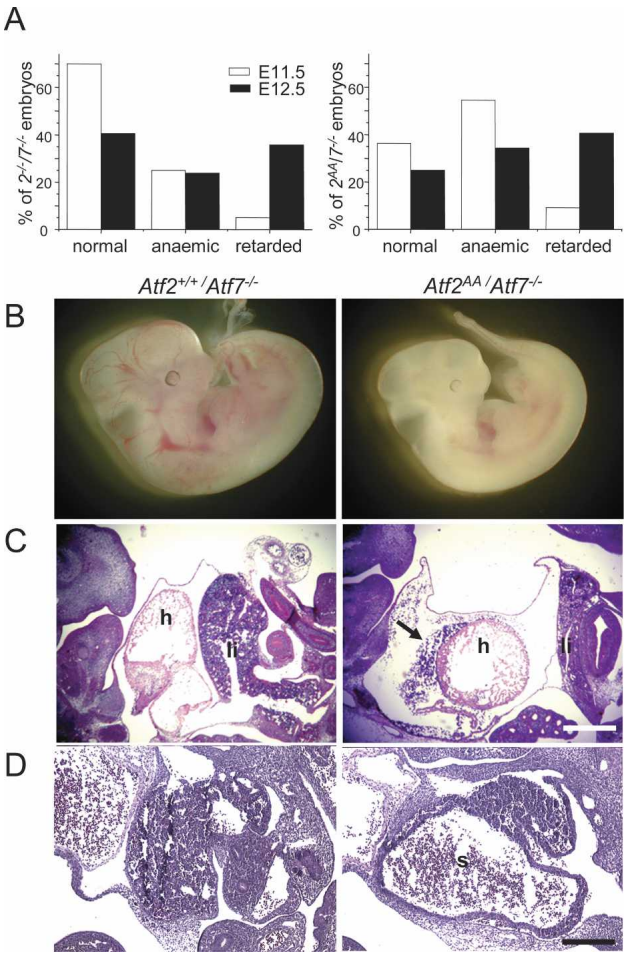

Figure 2. ATF2/7 mutant combinations lead to defects in developing heart and liver. (*A*) $Atf2^{-/-}/Atf7^{-/-}$ and $Atf2^{AA}/Atf7^{-/-}$ mutants at E11.5 and E12.5 were scored according to the severity of their defects between appearance indistinguishable to ATF2 wild-type or heterozygous embryos (normal), pale appearance without striking difference in developmental stage (anemic), or severe developmental abnormalities and arrest (retarded). (*B*) Comparison between normal $Atf2^{+/+}/Atf7^{-/-}$ embryo (*left*) and developmentally retarded $Atf2^{AA}/Atf7^{-/-}$ mutant (*right*) at E12.5. Bar, 50 µm. (*C*) Haematoxilin and eosin (H&E) staining of E12.5 corresponding sections from $Atf2^{+/+}/Atf7^{-/-}$ embryos (*left*) and $Atf2^{AA}/Atf7^{-/-}$ embryos (*right*). Heads are situated to the *left*. Defects in double mutant embryos include hypoplasia of the liver (li) and heart (h), often accompanied by large pericardial spaces and cardiac hemorrhages (arrow). Bar, 25 µm. (*D*) H&E staining of E12.5 embryos. In contrast to $Atf2^{+/+}/Atf7^{-/-}$ embryos (*left*), livers in $Atf2^{AA}/Atf7^{-/-}$ embryos (*right*) are often dysplastic with large sinuses (s) apparent. Bar, 10 µm.

the phenotype increasing between E11.5 and E12.5 (Fig. 2A). In both mutant combinations, placenta size as well as blood flow through the umbilical chord was found to be comparable with that in control embryos at these developmental stages. Furthermore, in placental sections no gross morphological defects were apparent in ATF2/7 mutants, and placental cell division appeared normal as shown by staining with the proliferation marker Ki67 (Supplementary Fig. S4). Therefore, the observed anemia is highly unlikely to be caused by defects in placental development. In addition, staining with vascular endothelial cell-specific markers vWF and CD31 revealed no significant loss of vascularization in mutant embryos (data not shown). In contrast, two striking deficiencies were found in the majority of mutant embryos. One was a significant reduction in heart size combined with the frequent observation of pericardial hemorrhages (Fig. 2C). The second phenotype affected the developing liver of double mutant embryos, where between E11.5 and E12.5 progressively increasing defects were observed with respect to liver size as well as liver architecture. Histological sections of embryos revealed that the livers of double mutant embryos were frequently rudimentary, occupying only a fraction of the abdominal areas compared with wild type (Fig. 2C). We also observed that, in some cases, livers were of normal size but contained considerable areas of tissue loss often compensated by large sinuses (Fig. 2D).

In liver tissues of double mutant embryos, cell density and tissue compactness appeared to be reduced, even at stages where the overall size of the mutant liver was not affected. We therefore asked whether this reduction in cell density was caused by reduced proliferation or whether a loss of liver cells had occurred due to cell death. Staining with the proliferation marker Ki67 showed that there was a moderate reduction of positively labeled cells in sections of ATF2/7 mutant embryos, but this was largely due to an overall decrease in cell density (Fig. 3A). In contrast, staining with antibodies detecting activated caspase 3 revealed a significant number of apoptotic signals in ATF2/7 mutant livers, while few apoptotic signals were found in control livers (Fig. 3B).

The embryonic liver consists of developing hepatocytes, but it is also the main organ of haematopoiesis during large periods of embryogenesis. We therefore asked whether the loss of liver cells by apoptosis in the ATF2/7 mutant embryos was restricted to specific cell types. Antibodies recognizing the fetal hepatocyte marker cytokeratin 18 revealed label-positive cells in ATF2/7 mutant embryos at E11.5, suggesting that, at least at this stage, developing hepatocytes were present (Fig. 3C). However, it was notable that cytokeratin 18 (CK18) staining revealed disorganized tissue architecture and that marker-positive cells were often rounded up or pycnotic. Apoptosis in mutant hepatocytes was confirmed by costaining of liver sections with antibodies against CK18 and activated caspase 3 (Fig. 3D). Thus, while developing hepatocytes emerge in ATF2/7 mutant livers at E11.5, loss of hepatocytes by apoptosis is a frequent occurrence. To confirm this observation we cultured fetal hepatocytes that were derived from control and mutant embryonic livers. Remarkably, far fewer CK18-positive cells were present in double mutant hepatocyte cultures compared with controls (Fig. 3E). In addition, mutant cultures revealed a significantly increased rate of activated caspase 3-positive signals (Fig. 3E), confirming that ATF2/7 mutant hepatocytes were highly apoptotic. Furthermore, the remaining cells ap-

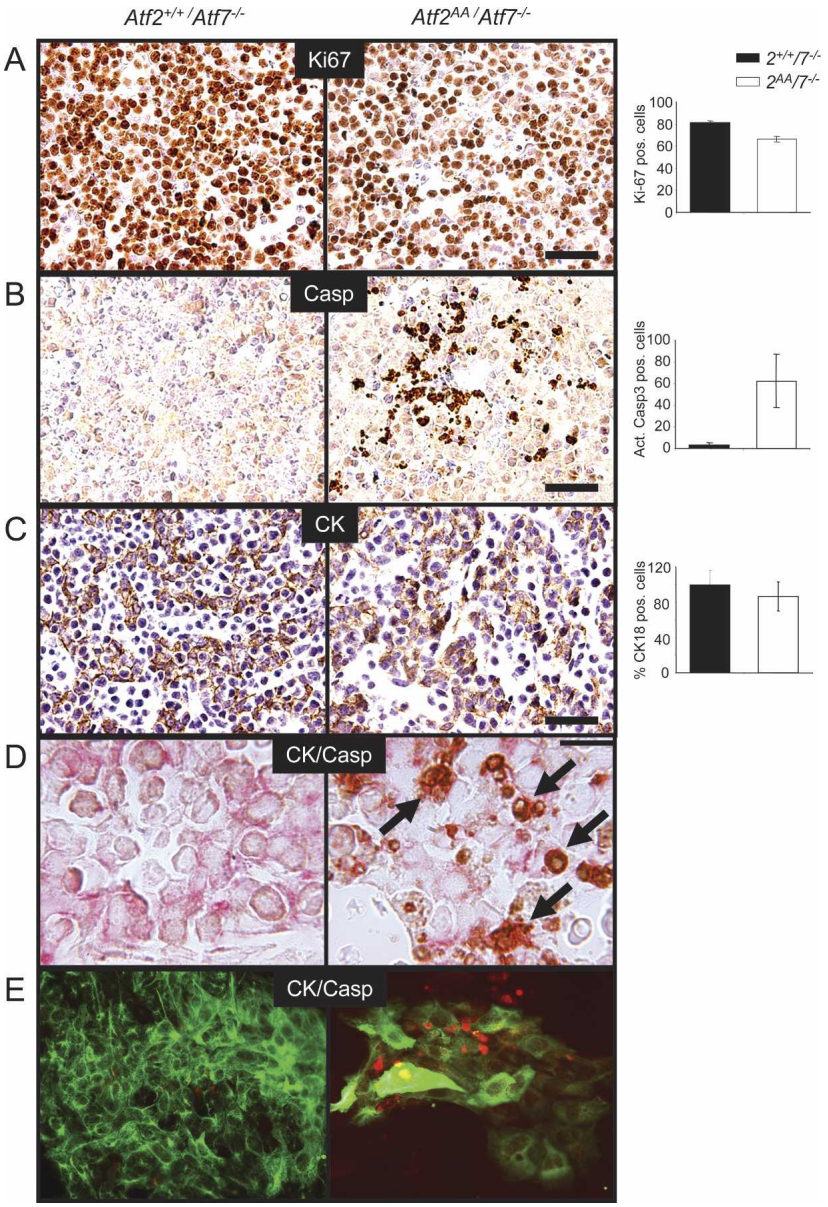

Figure 3. Apoptotic defects in ATF2/7 mutant fetal liver cells. $Atf2^{+/+}/Atf7^{-/-}$ samples are shown at the *left*, and $Atf2^{AA}/Atf7^{-/-}$ samples are shown at the *right*. Signal quantitation and statistical analysis were done on comparative fields of at least three sectioned livers. (*A–C*) Immunostainings were visualized by alkaline phosphatase (AP) staining (brown) and Gill 1× haematoxilin counterstaining of nuclei (blue). Bars, 2.5 µm. (*A*) Ki67 staining shows that while overall cell density is reduced, proliferation is ongoing in double mutant embryos. The graph indicates a small reduction in proliferating cells in double mutants ($P < 0.01$). (*B*) Activated caspase 3 (Casp) staining reveals excessive apoptotic activity in mutant liver sections. The graph indicates the average occurrence of apoptotic signals per liver section ($P < 0.01$). (*C*) Cytokeratin 18 (CK) staining (brown) reveals the presence of hepatoblasts in mutant sections. Many positive signals appear to be in small, rounded up cells. The graph shows the relative number of mutant CK18-positive cells as percentage of controls (n.s.). (*D*) Double antibody staining for CK18 (HRP, red) and activated caspase 3 (AP, brown) reveals apoptosis in hepatoblasts (arrows). (*E*) Immunofluorescence of fetal hepatocytes (CK18, green) in culture. Mutant cells are far reduced in number compared with control hepatocytes, mostly displaying large cytoplasms and associated with high apoptotic activity (activated caspase 3, red).

peared abnormally large and senescent. Staining for acidic β-galactosidase activity confirmed that cellular senescence occurred frequently in ATF2/7 mutant hepatocyte cultures but not in control cultures (see Fig. 6B, below).

The other prominent cell types in the developing liver consists of haematopoietic precursor cells. The observation of reduced liver size and frequent anemia in double mutant embryos prompted us to further investigate possible defects in haematopoietic, and especially erythropoietic, activities. Indeed, staining against the erythroid cell marker Ter119 revealed a significant reduction in marker-positive cells in double mutant livers (Fig. 4A). In addition, while in control sections erythroid cells were large and found in clusters, in mutant sections they were frequently single and small. In spite of the reduced number, proliferation is comparable between control and double mutant Ter119-positive cells (Fig. 4B). Therefore, the scarcity as well as the appearance of Ter119-labeled cells in double mutant livers could indicate apoptotic activity and correlates with the loss of erythroid lineage cells. Apoptosis in mutant erythroid cells was confirmed by double staining with Ter119 and active caspase 3 (Fig. 4C).

To confirm the loss of erythroid cells, protein was extracted from control and double mutant livers. While no difference was found in the levels of erythropoietin (data not shown), the levels of erythropoietin receptor, Epo-R, was significantly reduced in double mutant extracts (Fig. 4D). It has previously been demonstrated that Epo-R is essential for the survival of erythroid lineage cells in the embryo (Socolovsky et al. 1999), and that it performs this function through inducing the expression of the anti-apoptotic factor Bcl-x_L. In addition to the loss of Epo-R, we also found significantly reduced Bcl-x_L levels in

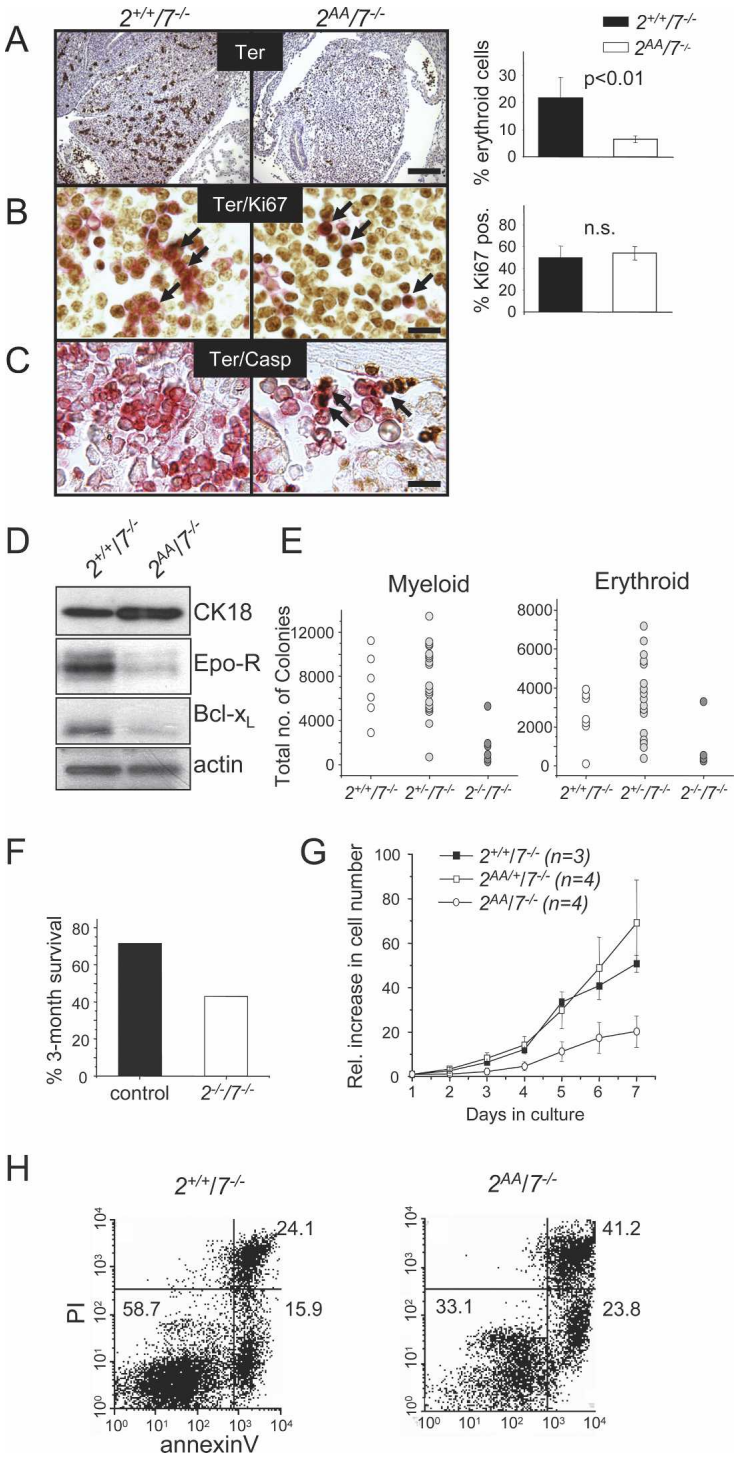

Figure 4. Haematopoietic defects in ATF2/7 mutant fetal livers. Sections of $Atf2^{+/+}/Atf7^{-/-}$ (*left*) and $Atf2^{AA}/Atf7^{-/-}$ (*right*) embryos (E11.5) are shown. Bars: *A*, 10 µm; *B*,*C*, 2.5 µm. (*A*) Staining of Ter119 (AP, brown) reveals great loss of erythroid cells in double mutant livers. The graph shows the percentage of erythroid (Ter119-positive) cells of the total cells in liver sections. (*B*) Staining of embryonic sections for Ter119 (HRP, red) and Ki67 (AP, brown). Arrows indicate double-stained cells present in controls and mutants. The graph shows the percentage of Ter119-positive cells expressing Ki67. (*C*) Double staining for Ter119 (HRP, red) and activated caspase 3 (AP, brown) reveals apoptosis in erythroid cells (arrows). (*D*) Western blot analysis of $Atf2^{+/+}/Atf7^{-/-}$ and $Atf2^{AA}/Atf7^{-/-}$ embryonic liver extracts at E12.5. Antibodies used were against cytokeratin 18 (CK18), erythropoietin receptor (Epo-R), Bcl-x_L, cJun, and β-actin. (*E*) Haematopoietic colony-forming cells from E12.5 livers. The total numbers of precursors per fetal liver were calculated by multiplying the average frequency of precursors in three dishes by the number of cells per fetal liver. Average numbers of myeloid colonies per liver were 6988 (standard deviation [SD], 1515) in $Atf2^{+/+}/Atf7^{-/-}$, 7812 (SD, 1333) in $Atf2^{+/-}/Atf7^{-/-}$, and 1857 (SD, 479) in $Atf2^{AA}/Atf7^{-/-}$ ($P < 0.005$). Average numbers of erythroid colonies per liver were 3542 (SD, 691) in $Atf2^{+/+}/Atf7^{-/-}$, 4053 (SD, 965) in $Atf2^{+/-}/Atf7^{-/-}$, and 1108 (SD, 309) in $Atf2^{AA}/Atf7^{-/-}$ ($P < 0.002$). Statistical analysis was performed using one-way ANOVA. (*F*) Survival rates of irradiated animals after injection of ATF2/7 mutant fetal liver cells. Control ($Atf2^{+/+}/Atf7^{-/-}$ and $Atf2^{+/-}/Atf7^{-/-}$, $n = 7$) or $Atf2^{-/-}/Atf7^{-/-}$ ($n = 7$) E12.5 fetal liver cells were administered to lethally irradiated PEP3 animals. The 3-mo survival rates of recipient animals are shown as the percentage of the input number. (*G*) Doubling indices of haematopoietic cells from control and double mutant embryonic livers in culture. Cells were seeded at 1×10^6 per milliliter and diluted to the same density every 48 h over 7 d. Graphs were plotted as averages of each represented genotype. (*H*) Apoptosis analysis of haematopoietic cells. Fetal liver cells were cultured in haematopoietic medium and stained for annexin V-FITC/PI and analyzed by FACS. The percentage rates of late apoptotic/dead cells (*top right* quadrant), live cells (*bottom left* quadrant), and early apoptotic cells (*bottom right* quadrant) are shown as the average of three clones of each analyzed phenotype.

double mutant extracts (Fig. 4D). In contrast, the levels of hepatocyte marker CK18 were slightly increased (Fig. 4D), indicative of altered ratios between hepatocytes and haematopoietic cells.

Increased apoptosis in ATF2/7 mutant haematopoietic cell cultures

We examined haematopoietic precursors in day 12.5 fetal livers in colony-forming cell assays and found that cells from $Atf2^{-/-}/Atf7^{-/-}$ livers produced a severely reduced total number of colonies compared with cells from control livers (Fig. 4E). This lack in colony-forming ability was apparent in both myeloid and erythroid precursors, suggesting that the defect affects both haematopoietic lineages. Similar results were obtained in $Atf2^{AA}/Atf7^{-/-}$, confirming the similarity of the different mutant combinations (data not shown). To further determine the loss of haematopoietic potential of double

mutant liver cells, we injected embryonic liver cells into lethally irradiated recipient animals. Significantly, only a minority of animals injected with double mutant liver cells showed long-term survival compared with animals injected with control cells (Fig. 4F). This further confirms a loss in the haematopoietic potential of ATF2/7 mutant liver cells.

To explore possible defects in haematopoietic precursor cells, we explanted fetal liver cells from control and mutant embryos and cultured them in serum-free medium supplemented with haematopoietic growth factors and cytokines. In these cultures, control cells ($Atf2^{+/+}$/$Atf7^{-/-}$ and $Atf2^{\Delta A/+}$/$Atf7^{-/-}$) were doubling cell numbers approximately every 24 h. In contrast, many $Atf2^{\Delta A}$/$Atf7^{-/-}$ cultures barely increased cell numbers over these periods (Fig. 4G), and in some mutant cultures, cell numbers were, in fact, reduced after 2–3 d of culturing. To confirm that the failure to increase cell numbers in mutant cultures was due to apoptosis, we stained cells with the apoptotic marker annexin V and analyzed them by FACS (Fig. 4H). We found, typically, that in control cultures, the majority of cells were alive as determined by propidium iodide (PI) uptake, as well as negative for annexin V. In contrast, in the mutant cultures the amount of dead (PI-positive) cells was significantly higher compared with the control cultures. Furthermore, a larger proportion of live cells was annexin V positive, indicating that, in double mutants, the lack of relative cell number increase in fetal liver cultures is caused by increased apoptosis. This experiment also indicates that the high rate of apoptosis in haematopoietic cells occurs independently of the same defect observed in hepatocytes, although the underlying mechanism might be the same.

Increased activated p38 in ATF2/7 mutant embryonic liver

To understand the mechanism by which cell loss is induced in the ATF2/7 mutant fetal livers, we analyzed apoptotic pathways that could be involved. Since mutations in the NFκB pathway lead to embryonic liver apoptosis (Beg et al. 1995; Rudolph et al. 2000) we assessed NFκB signaling by measuring the expression of two anti-apoptotic NFκB target proteins, XIAP and $cFLIP_L$. Both proteins were present at comparable levels between control and double mutant liver extracts, suggesting that NFκB anti-apoptotic signaling is normal (Fig. 5A). Likewise, levels of proapoptotic Bcl-2 family members Bax and Bid appeared unaltered in double mutant extracts. Interestingly, among the initiator caspases, levels of pro-caspase 9 were the same between controls and mutants, while the levels of pro-caspase 8 were greatly diminished in double mutant extracts. Thus, caspase 8 processing indicates that receptor-mediated caspase activation is involved in the observed apoptotic process. The germline deletion of *cJun* also leads to embryonic liver defects. However, no differences in cJun protein levels were found between control and double mutant embryonic livers (Fig. 5A).

Next we analyzed the stress-activated MAPKs whose activities are associated with regulation of apoptosis. In immunohistochemical stainings of embryonic sections we found no remarkable difference in the level of JNK and p38 between control and double mutants (data not shown). In contrast, while no difference in phosphorylated (Thr183/Tyr185) JNK was detected, phosphorylated (Thr180/Tyr182) p38 was significantly increased in livers of double mutant embryos (Fig. 5B). Interestingly, such hyperactivation was most evident in the liver, with no significant differences in the level of phosphorylated p38 between wild-type and mutant embryos overall. To determine the cell type in which p38 was hyperphosphorylated we stained embryonic sections for P-p38 together with lineage markers Ter119, or cytokeratin18 (Fig. 5C). In double mutant livers, at least a subset of the remaining Ter119-positive cells strongly stained for P-p38 compared with controls. In livers where significant tissue damage was apparent, P-p38 staining mainly correlated with CK18-labeled cells, while Ter119 staining was mostly associated with erythrocytes present in sinuses. Therefore, in double mutant livers both erythroid cells and hepatoblasts express hyperphosphorylated p38.

The presence of hyperactive p38 in double mutant livers was confirmed in protein extracts from control and double mutant embryonic livers, where no differences in amounts of total p38 were apparent, whereas P-p38 was significantly enhanced in the double mutant (Fig. 5D). Quantitatitively, P-p38 doubled in ATF2/7 mutant extracts (Fig. 5D), which reflects an average of all cells present in the livers and has to be seen in the context of significantly higher P-p38 levels observed in specific cells by immunohistochemical staining (Fig. 5B,C). Furthermore, the increase in p38 activation was not a result of a general stress response, because levels of phosphorylated JNK appeared, in fact, slightly decreased in mutant extracts, while phosphorylation level of upstream kinases MKK3, MKK4, and MKK6 appear similar between mutant and control extracts (Fig. 5D). No significant differences in P-p38 levels were observed in extracts of ATF2 single mutant livers (Supplementary Fig. S5), confirming that p38 hyperphosphorylation was associated with the loss of both ATF2 and ATF7.

Enhanced or persistent p38 activity may result in the high levels of liver cell apoptosis observed in double mutant embryos. If this was the case, we would expect that inactivation of phosphorylated p38, through the application of chemical inhibitors, should lead to greater cell survival. To test this hypothesis we cultured haematopoietic cells from control and double mutant livers in the absence or presence of a p38-specific inhibitor at concentrations that have been shown to be highly effective and specific (Davies et al. 2000). In control cultures, addition of a p38 inhibitor delivered no reduction in the level of apoptotic (annexin V-positive) cells (Fig. 6A). In contrast, in double mutant cultures the addition of the p38 inhibitor led to a reduction in apoptotic cells to levels comparable with control cultures. This result supports the notion that high levels of p38 activity are largely responsible for the high levels of apoptosis in the

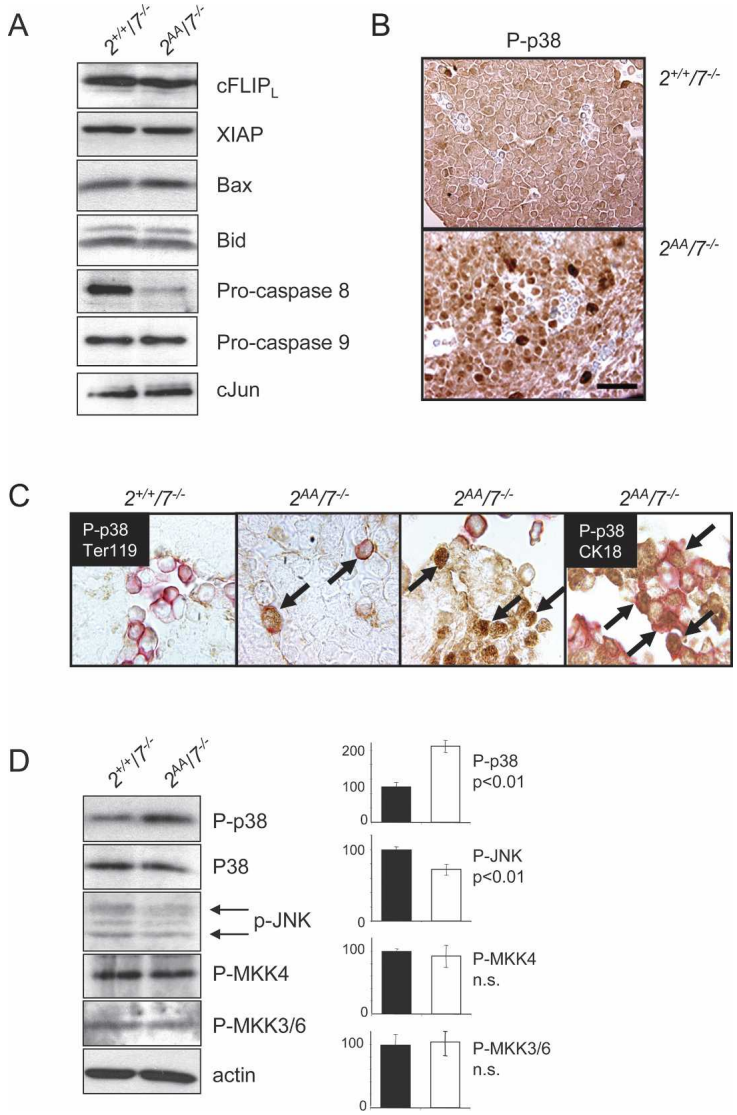

Figure 5. Apoptotic regulators in ATF2/7 mutant livers. (*A*) Western blot analysis of $Atf2^{+/+}/Atf7^{-/-}$ and $Atf2^{AA}/Atf7^{-/-}$ embryonic liver extracts. Proteins were probed with antibodies against cFLIP, XIAP, Bax, Bid, Pro-caspase 8, Pro-caspase 9, and cJun. (*B*) AP staining of P-p38 in $Atf2^{+/+}/Atf7^{-/-}$ (*top*) and $Atf2^{-/-}/Atf7^{-/-}$ (*bottom*) paraffin-embedded embryonic liver section (E12.5). Nuclei are stained with haematoxilin (blue). Bar, 2.5 µm. (*C*) Double staining of embryonic sections for peroxidase-labeled P-p38 (brown) and AP-labeled (red) Ter119 (first through third panels from *left*) or CK18 (fourth panel). Arrows indicate strong P-p38 signals in erythroid cells (third panel) or hepatocytes (fourth panel) in double mutants. (*D*) Western blot analysis of $Atf2^{+/+}/Atf7^{-/-}$ and $Atf2^{AA}/Atf7^{-/-}$ embryonic liver extracts (E12.5). Densitometric measurements were taken from Western blot analyses of three independent embryo litters and averages were plotted. Staining against pan-p38 and P-p38 reveal increased levels of the activated form of the kinase, while overall protein levels are constant. A small but significant decrease in phosphorylated JNK levels (p54 and p46, arrows) was apparent. No significant changes were apparent in phosphorylation status of MKK4 and MKK3/6.

haematopoietic compartment of double mutant livers. Unrestricted p38 activity could also be responsible for the increased apoptosis and occurrence of premature senescence in ATF2/7 mutant embryonic hepatocytes (Fig. 3E). In contrast to wild-type controls, ATF2/7 mutant hepatocytes showed frequent senescence-associated β-Gal staining (Fig. 6B), consistent with their large appearance and failure in growth (Fig. 3E). Addition of the p38 inhibitor suppressed staining and, hence, premature senescence, and led to increased numbers of hepatocytes in culture (Fig. 6B). Therefore, we conclude that negative regulation of p38 activity is important for survival and growth of embryonic hepatocytes.

ATF2 provides a negative feedback mechanism for p38 regulation

The observation that p38 kinase activity is up-regulated as a consequence of loss of ATF2 phosphorylation suggests the existence of a regulatory feedback mechanism mediated by ATF2. We therefore analyzed potential ATF2 targets among phosphatase genes that may regulate the activity of p38. In ATF2/7 mutant embryonic livers, enhanced phosphorylated p38 correlates with significantly reduced levels of the dual specificity phosphatase 1 (DUSP1, MKP1), a known MAPK phosphatase that regulates JNK and p38 (Fig. 6C). Interestingly, the *Dusp1* gene, as well as a number of other genes encoding dual-specificity phosphatases such as DUSP5, DUSP8, and DUSP10 (MKP5), contain consensus CRE elements in their proximal promoters (Fig. 6D). RNA analysis from $Atf2^{+/+}/Atf7^{-/-}$, $Atf2^{-/-}/Atf7^{-/-}$ (data not shown) and $Atf2^{AA}/Atf7^{-/-}$ fetal livers revealed that while a number of liver-specific transcripts, including albumin and hepatocyte growth factor (HGF), or other AP-1 factors—e.g., cJun—were not affected by the ATF2/7 mutations, the levels of *Dusp1*, *Dusp5*, *Dusp8*, and *Dusp10* mRNAs were significantly reduced in double mutants (Fig. 6E).

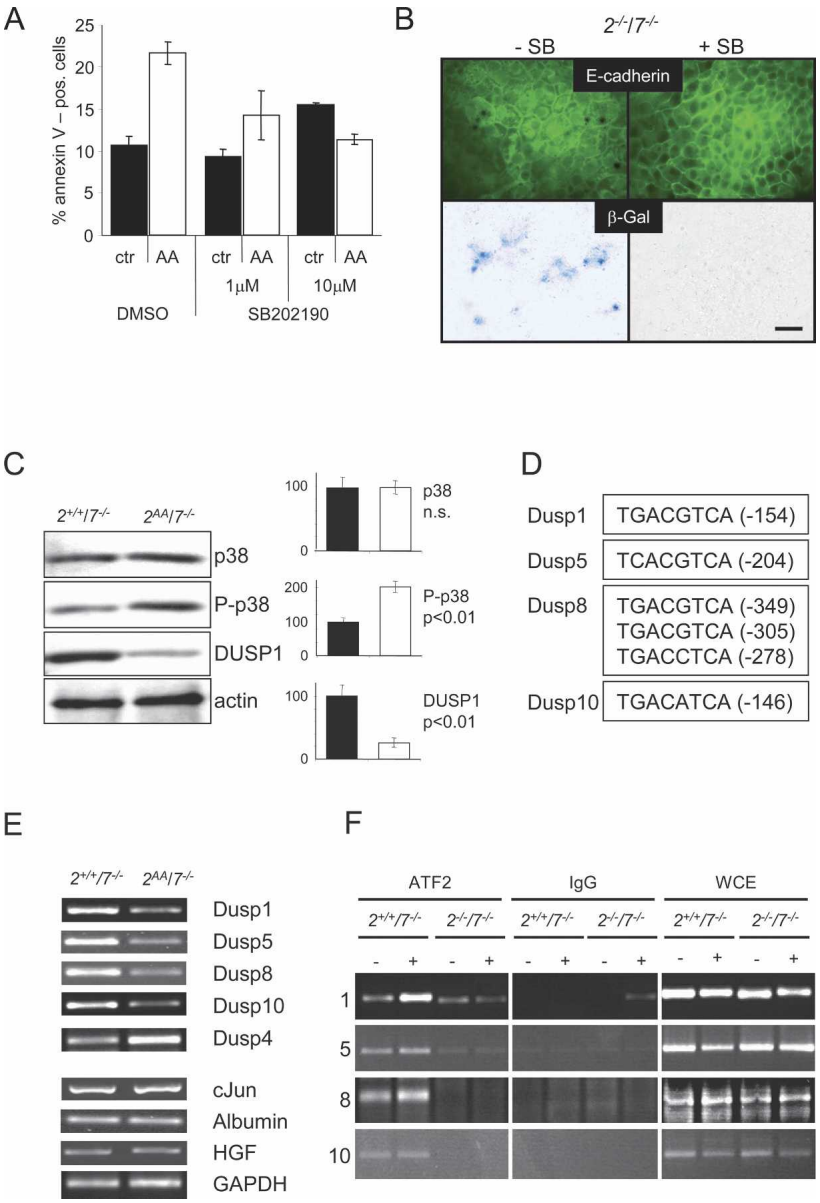

Figure 6. Regulation of p38 activity controls fetal liver apoptosis. (*A*) FACS analysis of $Atf2^{+/+}/Atf7^{-/-}$ and $Atf2^{AA}/Atf7^{-/-}$ haematopoietic cultures derived from fetal livers. Cultures were mock-treated or continuously treated with p38 inhibitor SB202190 (1 or 10 μM) over 4 d, stained with annexin V-FITC and PI, and analyzed by flow cytometry. The graph shows the average distribution of live (PI-negative), nonapoptotic (annexin V-low) versus apoptotic (annexin V-high) cells from three independent cell lines of control cells (black bar) and double mutant cells (white bar). (*B*) p38-dependent premature cellular senescence of ATF2/7 mutant hepatocytes in culture. Primary $Atf2^{-/-}/Atf7^{-/-}$ fetal hepatocytes were cultured for 5 d in the absence (–) or presence (+) of SB202190 (2 μM) and stained for senescence-associated β-galactosidase. Mock-treated cells frequently stain blue, while p38-inhibitor-treated cells rarely stain blue. *Top* panels show fluorescent staining for E-cadherin (green) to identify hepatocytes. Bar, 2.5 μm. (*C*) Western blot analysis of $Atf2^{+/+}/Atf7^{-/-}$ and $Atf2^{AA}/Atf7^{-/-}$ fetal livers reveals loss of DUSP1 protein, correlating with increased levels of P-p38 in ATF2/7 mutant extracts. Densitometric quantification and statistical significance is shown on the *right*. β-actin is shown as loading control. (*D*) Schematic view of mouse dual-specificity phosphatase gene promoters. Putative ATF/AP-1-binding sites and their positions with respect to transcription start sites are shown. (*E*) RT–PCR analysis of RNA extracts from $Atf2^{+/+}/Atf7^{-/-}$ and $Atf2^{AA}/Atf7^{-/-}$ embryonic livers. PCR primer pairs were designed to span intronic sequences where possible. (*F*) ChIP of promoter sequences of dual-specificity phosphatase genes *Dusp1* (*1*), *Dusp5* (*5*), *Dusp8* (*8*), and *Dusp10* (*10*) before and after anisomycin treatment (aniso, 10 μg/mL). ATF2 and control IgG antibodies were used. Whole-cell extracts (WCE) were used as PCR controls.

Furthermore, in ChIP analyses, CRE-containing promoter sequences of *Dusp1, Dusp5, Dusp8,* and *Dusp10* were amplified efficiently in $Atf2^{+/+}/Atf7^{-/-}$ but not in $Atf2^{-/-}/Atf7^{-/-}$ extracts, confirming that the transcription of these phosphatase genes was regulated by the direct binding of ATF2 to their promoters (Fig. 6F). Interestingly, the expression of another phosphatase gene, *Dusp4* (*Mkp2*), was found hyperinduced in ATF2/7 mutant livers, suggesting that this phosphatase gene is negatively regulated by ATF2 (Fig. 6E). We also tested the requirement of ATF2 for MAPK regulation in primary MEFs. After stress induction with PMA, ATF2/7 mutant MEFs showed a marked increase of phosphorylated p38 compared with ATF2 wild-type control cells (Fig. 7A). Hyperphosphorylation was restricted to p38 since no differences were found in the phosphorylation status of JNK and ERK. In addition, no significant differences were found in the phosphorylation status of upstream MAPK kinases, including MEK1, MKK3/6, MKK4, and MKK7 (Fig. 7A). Therefore, deregulated p38 phosphorylation was not associated with increased activity of upstream kinases. We also found that a number of Dusp genes, some of which are direct targets of ATF2 (Fig. 6F) are induced in MEFs following stress or serum stimulation (data not shown). To determine whether this induction is dependent on ATF2/7 activity, we compared induction patterns of these genes in $Atf2^{-/-}/Atf7^{-/-}$ MEFs transformed with a control retrovirus or a retrovirus containing the wild-type ATF2 gene (Fig. 7B). Expression of ATF2 in the ATF2/7 mutant cells resulted in enhanced induction of some of these genes after stress (*Dusp1, Dusp2,* and *Dusp8*) or serum stimulation (*Dusp1, Dusp2, Dusp8,* and *Dusp10*). Thus, phosphatase genes found to be regulated by ATF2 in the liver, and in addition *Dusp2,*

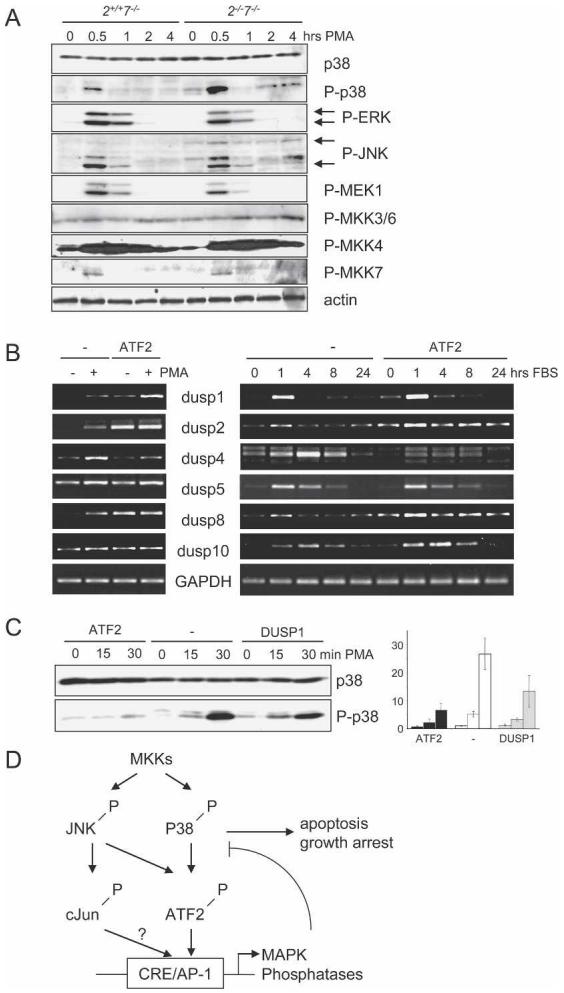

Figure 7. ATF2 restricts p38 phosphorylation in MEFs. (*A*) Primary $Atf2^{+/+}/Atf7^{-/-}$ and $Atf2^{-/-}/Atf7^{-/-}$ MEFs before and after stress (PMA, 1 μg/mL). Phosphorylation levels of p38 (T180/Y182), ERK (T202/Y204), JNK (T183/Y185), MKK3/6 (S189/207), MKK4 (S257/T261), and MKK7 (S271/T275) were determined using phospho-specific antibodies. β-actin is shown as loading control. (*B*) RT–PCR analysis of RNA extracts of immortalized $Atf2^{-/-}/Atf7^{-/-}$ MEFs transformed with control retrovirus pBP (–) or pBP expressing wild-type ATF2. Expression of DUSP genes was analyzed upon stress induction (PMA 1 μg/mL, 20 min) or FBS (10%). (*C*) Phosphorylation levels of p38 after stress induction (PMA, 1 μg/mL) in $Atf2^{-/-}/Atf7^{-/-}$ MEFs transformed with retrovirus pBP as control (–), or pBP expressing ATF2 or DUSP1. Total p38 levels are shown as loading control. The graph shows the levels of P-p38 relative to total p38 as the averages of three independent experiments. (*D*) Model of feedback mechanism involving activated ATF2 regulating p38 activity. MKKs activate JNK and p38 by phosphorylation. Among MAPK targets are cJun and ATF2 (and ATF7), which regulate the expression of MAPK phosphatases. Failure in their activation leads to hyperactive p38, which, at least in the developing liver, is detrimental to cell survival and growth.

require ATF2 for maximal activation by stress or growth factors also in MEFs. In contrast, re-expression of ATF2 leads to reduced activation of *Dusp4* expression after stress or serum induction (Fig. 7B) confirming its negative regulation by ATF2 as observed in the embryonic liver. Re-expression of either ATF2 or DUSP1 in ATF2/7 mutant MEFs significantly reduced levels of stress-induced p38 phosphorylation (Fig. 7C). We therefore conclude that the stress-induced hyperphosphorylation of p38 is likely to be a direct consequence of loss of ATF2/7-dependent phosphatase activity.

Discussion

Previous mouse knockout studies have revealed essential functions for ATF2 in mouse development and inflammatory response (Reimold et al. 1996, 2001; Maekawa et al. 1999). Here we show that N-terminal phosphorylation is an absolute necessity for ATF2 function in vivo, because a germline mutation in two MAPK phosphorylation sites of ATF2 leads to severe developmental defects that are comparable with complete loss of its DNA-binding ability. $ATF2^{AA}$ is stable and is able to bind to DNA and therefore homodimerization or heterodimerization with other leucine zipper proteins appears to be functional. In contrast to other AP-1 proteins such as cJun, cFos, and ATF3, which are induced transcriptionally after cellular stimulation, ATF2 is ubiquitously expressed and its activation occurs predominantly at the post-translational level through phosphorylation by stress and mitogen-stimulated kinases (Gupta et al. 1995; Ouwens et al. 2002). This provides a rapid mechanism to adjust gene expression to changes in the cellular environment, such as growth stimulation or stress conditions.

As is the case with other components of the MAPK signaling pathway and AP-1 transcription factors, redundancy appears to be a feature of the ATF2 family and novel phenotypes emerge as a result of combinations of mutations. While deletion of ATF2 function leads to lethality that occurs soon after birth, embryonic development, on the whole, is completed (Maekawa et al. 1999; this study). Novel and essential functions for ATF2 in development only become apparent when its closest homolog, ATF7, is also mutated. These functions include heart development as well as protection of fetal hepatocytes and haematopoietic precursors from apoptotic cell death. The finding that the phenotypes seen in the ATF2 phosphorylation mutant mirrors those seen in the DNA-binding mutant confirms that ATF2 is an essential effector of MAPK signaling.

Mouse knockout studies have revealed that components of the MAPK pathways are essential for embryonic liver development. Deficiency in MKK4 (SEK1), a regulatory kinase for JNK and p38 (Derijard et al. 1995; Lin et al. 1995), leads to embryonic lethality between E11.5 and E12.5, and severe defects in liver development are observed (Ganiatsas et al. 1998; Nishina et al. 1999). $Mkk4^{-/-}$ liver buds are significantly smaller at E11.5 compared with wild type, and this coincides with significantly increased liver cell apoptosis and a greatly reduced number of parenchymal hepatocytes. In the developing liver, MKK4 is assumed to function via cJun, based on the findings that cJun is activated by MKK4 through

JNK (Derijard et al. 1994; Sanchez et al. 1994; Lin et al. 1995). In addition, the *Mkk4* knockout is reminiscent of the *cJun* knockout, which is embryonic lethal and displays severe liver defects and significant loss of hepatoblasts (Hilberg et al. 1993; Johnson et al. 1993). However, close examination of the liver defect in $cJun^{-/-}$ revealed that the onset of the hepatocytic defect due to apoptosis and lack of proliferation does not occur at a significant level before E13 (Eferl et al. 1999), considerably later than the liver apoptosis observed in $Mkk4^{-/-}$. In addition, mutation of the N-terminal phosphorylation sites Ser63 and Ser73 has no effect on liver development (Behrens et al. 1999). This would argue against cJun being the prime responder of MKK4/JNK signaling, although the possible role of the two additional phosphorylation sites at Thr91 and Thr93 has not been determined.

Both $Atf2^{-/-}/Atf7^{-/-}$ and $Atf2^{AA}/Atf7^{-/-}$ embryos share many of the features that are observed in $Mkk4^{-/-}$ and $cJun^{-/-}$ knockouts, including loss of liver tissue during mid-gestation concomitant with severe apoptosis in liver cells. Since, in some circumstances, *cJun* is a transcriptional target of ATF2, the phenotype in the ATF2/7 mutant livers could be explained by the lack of cJun in these cells. However, we found that cJun levels were comparable between control and double mutant livers (Figs. 5A, 6E). It is therefore more likely that ATF2 (and ATF7) is an essential downstream effector of activated MKK4 in the developing liver, and that it acts as a heterodimer with cJun on AP-1-induced gene promoters, securing the survival of developing liver cells. Compared with cJun, ATF2-dependent liver function has an earlier onset, with rates and severity of the defects in the ATF2/7 double mutants closely resembling those found in $Mkk4^{-/-}$ livers. In addition, N-terminal phosphorylation of ATF2 is essential for liver cell survival. The difference in onset of the liver apoptosis in $cJun^{-/-}$ may be explained by the presence of other Jun family proteins, such as JunB or JunD, which could serve as dimerization partners of ATF2 at earlier stages of development.

ATF2/7 double mutant embryos are severely anemic, and a loss of Ter119-positive, erythroid lineage cells is observed in mutant embryonic livers. In contrast, while $Mkk4^{-/-}$ embryos are also severely anemic, no significant defect in haematopoietic precursors is apparent, and $Mkk4^{-/-}$ fetal liver cells can reconstitute haematopoiesis in recipient animals (Ganiatsas et al. 1998; Nishina et al. 1999). We found that cultures of haematopoietic precursor cells derived from ATF2/7 mutant fetal livers grow abnormally slowly, largely due to loss of cells by apoptosis. In addition, in embryonic liver extracts from ATF2/7 mutant embryos p38 activity is significantly up-regulated. We also showed that chemical inhibition of p38 activity in haematopoietic cultures reverts the apoptotic phenotype of the double mutant cells, supporting the hypothesis that p38 hyperactivity could be a primary cause of the observed apoptosis in ATF2/7 mutant livers. Embryonic erythropoiesis is a multistep process, and it has been established that protection of erythroid precursor cells from apoptosis is an essential regulatory mechanism (Socolovsky et al. 1999). Haematopoietic cytokines, and specifically erythropoietin, activate MAPKs, including p38. Deletion of p38 in the mouse results in defects in placental organogenesis (Adams et al. 2000) and lung homeostasis (Ventura et al. 2007). A potential role in erythropoiesis via the regulation of erythropoietin expression has also been described (Tamura et al. 2000), although this is a not a frequent phenotype and has not been consistently seen (Adams et al. 2000). In contrast, in many cell types including erythroid progenitor cells, p38 activity is also associated with induction of apoptosis (Somervaille et al. 2003; Porras et al. 2004). It is therefore conceivable that p38 activity, depending on its strength and duration, induces differentiation, but also apoptosis.

In embryonic livers ATF2 regulates the levels of active p38 through the direct transcriptional activation of MAPK-specific phosphatases such as DUSP1, DUSP5, DUSP8, and DUSP10. Previously, the *Dusp1* promoter was identified as one of a number of promoters that directly interacted with ATF2 and cJun upon cisplatin treatment (Hayakawa et al. 2004).

Interestingly, primary fibroblasts derived from mice lacking DUSP1 exhibit hyperactivation of p38 in response to serum addition or stress conditions (Wu and Bennett 2005). In addition, DUSP1-deficient cells are hypersensitive to stress-induced apoptosis, and the enhanced level of cell death is rescued by addition of a p38-specific chemical inhibitor, but not by a JNK-specific inhibitor, thus demonstrating a critical role for DUSP1 in the negative regulation of p38 in response to stress to promote cell survival in cultured fibroblasts. Many of the DUSPs regulated by ATF2 have been implicated in the regulation of JNK and ERK activation as well as p38 activation. Nevertheless, in the ATF2/7 mutant embryonic liver we specifically see hyperactivation of p38. The feedback regulation of MAPK signaling via DUSPs is likely to depend upon the amalgam of phosphatase activities, which may vary from one cell type to another and in response to different signals. Loss of ATF2/7 leads to profound changes in the overall pattern of DUSP expression with many being down-regulated, but at least one, DUSP4, being up-regulated. While DUSP4 (MKP2) interacts with all three MAPK families in vitro, a number of reports show that it selectively targets JNK for dephosphorylation in vivo (Paumelle et al. 2000; Cadalbert et al. 2005). We hypothesize that in the embryonic liver cells, this change in overall pattern has a significant effect on p38 activation, whereas the effect on JNK is minimal, possibly due to the compensating activity of DUSP4. Furthermore, the specificity toward p38 may not be the case in all cell types and under all conditions, because the overall pattern of DUSP activity will vary. Indeed, we have observed conditions with ATF2/7 mutant fibroblasts in which JNK, p38, and in addition ERK, are hyperphosphorylated (data not shown).

We propose a model whereby p38 and ATF2 are connected in a negatively acting feedback loop through the activation of p38-specific phosphatases (Fig. 7D). A failure in this regulatory loop may lead to deleterious levels

in activity of a potent kinase. Such a negative feedback loop between AP-1 proteins and their upstream kinases has been shown after stress induction in *Schizosaccharomyces pombe* (Wilkinson et al. 1996), and in *Drosophila* development (Martin-Blanco et al. 1998). We are presently examining whether a failure in this mechanism is involved in other ATF2/7 mutant phenotypes, such as the defect observed in the developing heart. RNA extracts from ATF2/7 mutant embryonic hearts also reveal reduced amounts of phosphatase genes (W. Breitwieser and N. Jones, unpubl.). It is therefore conceivable that the interplay between p38 and ATF2 signaling is also important for embryonic heart development. Furthermore, in humans, p38 activity is associated with a long list of medical conditions such as inflammation or cardiac muscle hypertrophy, and two recent reports using mouse knockouts have shown that p38 can suppress K-ras-induced tumourigenesis in the lung and chemical-induced tumourigenesis in the liver (Hui et al. 2007; Ventura et al. 2007). A closer examination of the activity of ATF2 in such circumstances may shed new light on the activity and regulation of these MAPKs.

Materials and methods

Generation of ATF mutant transgenic mice

Atf2 genomic sequences were isolated by screening a 129/ola mouse cosmid library (RZPD). ATF2^{AA} mutant clones were generated by in vitro mutagenesis (Promega) and insertion of genomic sequences into *pPGKneobpAlox2PGKDTA* (kindly received from Frank Gertler, Massachusetts Institute of Technology, Cambridge, MA). Linearized, wild-type, and mutated targeting vectors were transfected into 129/ola embryonic stem cells and selected for G418 resistance. Transgenic animals were produced by blastocyst injection and offspring mice were backcrossed at least six times with C57 Bl/6 mice to produce isogenic lines. *Atf2*$^{AA/+}$ mice were crossed with *PGK1-Cre* transgenic mice (with kind permission from Peter Lonai, Weizmann Institute, Rehovot, Israel) to excise the neomycin selection marker from the ATF2 genomic sequence by Cre-loxP recombination.

Primary cell culture and apoptosis analysis

MEFs were cultured in DMEM (Invitrogen) and 10% fetal bovine serum (FBS) (Autogen Bioclear). For in vitro hepatocyte cultures, E11.5 and E12.5 fetal liver cells were dissociated in liver digest medium (Invitrogen) and plated in gelatine-coated dishes in hepatocyte culture medium containing 10% FBS, 2 mM glutamine, 1× nonessential amino acids, insulin–transferrin–selenium X supplement (all Invitrogen), and 10^{-7} M dexamethasone (Sigma-Aldrich). Fetal haematopoietic cells were cultured in serum-free medium (Stem-pro-34, Invitrogen) supplemented with 2 mM glutamine, 0.2 mg/mL transferrin (Roche Applied Science), 0.004% monothioglycerol, 25 µg/mL ascorbic acid (all Sigma-Aldrich), 5 ng/mL IL-11, 5 ng/mL IL-6, 25 ng/mL IGF-1, 3 ng/mL GMCSF (all R&D Systems), Kit-ligand (1% conditioned medium), and Il-3 (1% conditioned medium). For apoptosis assays, haematopoietic cells were incubated with annexin V and PI (Sigma-Aldrich) and were analyzed by FACS.

Immunohistochemistry and immunofluorescence

Embryos were fixed overnight in 4% buffered formalin. Four-micron sections were produced from paraffin-embedded samples and antigen retrieval was carried out according to antibody specification. For immunofluorescence, cell cultures were fixed in 3% paraformaldehyde/PBS for 30 min, permeabalized with 0.1% Triton X-100/PBS for 10 min, and blocked in 5% skimmed milk/PBS for 10 min before antibody incubation overnight in 5% FCS/PBS. Primary antibodies used are specified in Supplementary Figure S7. Senescence staining was done overnight at 37°C using Senescence β-Galactosidase Staining Kit (Cell Signaling).

Colony assays and bone marrow reconstitution

Myeloid and erythroid haematopoietic precursors present in fetal liver were evaluated by plating 10,000 fetal liver cells per milliliter of a 1% methylcellulose solution containing 10% plasma-derived serum and the cytokines Kit-ligand (1% conditioned medium), thrombopoietin (1% conditioned medium), 2 U/mL erythropoietin, 5 ng/mL IL-11, 3 ng/mL GM-CSF, IL-3 (1% conditioned medium), 10 ng/mL M-CSF, and 10 ng/mL IL-6. Cultures were maintained at 37°C and 5% CO_2, and colonies were counted after 7–10 d. For reconstitution assays, 10- to 12-wk-old PEP-3 mice were irradiated with a dose of 10 Gy (X-ray, 2.1 cGy/min) to ablate bone marrow, and fetal liver cells were injected i.v. Any animal showing adverse effects was humanely killed. All animal work was performed following strict ethical guidelines and within the limits of a licence granted by the Home Office according to the Animals (Scientific Procedures) Act 1986.

RNA, protein, and chromatin analysis

RNA was extracted from embryonic livers using PicoPure RNA Isolation Kit (Arcturus) or from MEFs using Trizol (Invitrogen) and was purified using RNeasy reagent (Qiagen); semiquantitative RT–PCR was performed using Reverse Transcription System (Promega) and Jumpstart PCR reagent (Sigma-Aldrich). The sequences for PCR primers are shown in Supplementary Figure S6.

Fetal liver protein was extracted using Cytobuster reagent (Novagen), was separated on 10% or 15% SDS-PAGE and blotted onto PVDF membranes (Millipore) and was visualized via ECL Detection Kit (Amersham). The primary antibodies used are specified in Supplementary Figure S7.

For ChIP analyses, MEFs were fixed in 1% formaldehyde. Extracts were sonicated and immunoprecipitated with ATF2 antibodies or with IgG control antibodies. Reverse cross-linking was performed overnight at 65°C in 1% SDS, and DNA was purified using PCR Purification Kit (Qiagen). PCR reactions were carried out in 35 cycles using the primers listed in Supplementary Figure S6.

Acknowledgments

We are grateful to the members of FACS laboratory for help in cell analysis, to members of the Molecular Biology Core Facility for help in sequencing and genotyping, to members of the Biological Resource Unit for help in animal maintenance and breeding, and to members of the Cellular and Molecular Pharmacology laboratory for sharing antibodies and reagents. We thank Caroline Wilkinson and Angeliki Malliri for critical reading of the manuscript, and members of the Cell Regulation laboratory for helpful discussions. We thank CRUK for funding of this project.

References

Adams, R.H., Porras, A., Alonso, G., Jones, M., Vintersten, K., Panelli, S., Valladares, A., Perez, L., Klein, R., and Nebreda,

A.R. 2000. Essential role of p38α MAP kinase in placental but not embryonic cardiovascular development. *Mol. Cell* **6:** 109–116.

Beg, A.A., Sha, W.C., Bronson, R.T., Ghosh, S., and Baltimore, D. 1995. Embryonic lethality and liver degeneration in mice lacking the RelA component of NF-κ B. *Nature* **376:** 167–170.

Behrens, A., Sibilia, M., and Wagner, E.F. 1999. Amino-terminal phosphorylation of c-Jun regulates stress-induced apoptosis and cellular proliferation. *Nat. Genet.* **21:** 326–329.

Behrens, A., Sabapathy, K., Graef, I., Cleary, M., Crabtree, G.R., and Wagner, E.F. 2001. Jun N-terminal kinase 2 modulates thymocyte apoptosis and T cell activation through c-Jun and nuclear factor of activated T cell (NF-AT). *Proc. Natl. Acad. Sci.* **98:** 1769–1774.

Benbrook, D.M. and Jones, N.C. 1990. Heterodimer formation between CREB and JUN proteins. *Oncogene* **5:** 295–302.

Bocco, J.L., Bahr, A., Goetz, J., Hauss, C., Kallunki, T., Kedinger, C., and Chatton, B. 1996. In vivo association of ATFa with JNK/SAP kinase activities. *Oncogene* **12:** 1971–1980.

Cadalbert, L., Sloss, C.M., Cameron, P., and Plevin, R. 2005. Conditional expression of MAP kinase phosphatase-2 protects against genotoxic stress-induced apoptosis by binding and selective dephosphorylation of nuclear activated c-jun N-terminal kinase. *Cell. Signal.* **17:** 1254–1264.

Chatton, B., Bocco, J.L., Goetz, J., Gaire, M., Lutz, Y., and Kedinger, C. 1994. Jun and Fos heterodimerize with ATFa, a member of the ATF/CREB family and modulate its transcriptional activity. *Oncogene* **9:** 375–385.

Davies, S.P., Reddy, H., Caivano, M., and Cohen, P. 2000. Specificity and mechanism of action of some commonly used protein kinase inhibitors. *Biochem. J.* **351:** 95–105.

Derijard, B., Hibi, M., Wu, I.H., Barrett, T., Su, B., Deng, T., Karin, M., and Davis, R.J. 1994. JNK1: A protein kinase stimulated by UV light and Ha-Ras that binds and phosphorylates the c-Jun activation domain. *Cell* **76:** 1025–1037.

Derijard, B., Raingeaud, J., Barrett, T., Wu, I.H., Han, J., Ulevitch, R.J., and Davis, R.J. 1995. Independent human MAP-kinase signal transduction pathways defined by MEK and MKK isoforms. *Science* **267:** 682–685.

Eferl, R. and Wagner, E.F. 2003. AP-1: A double-edged sword in tumorigenesis. *Nat. Rev. Cancer* **3:** 859–868.

Eferl, R., Sibilia, M., Hilberg, F., Fuchsbichler, A., Kufferath, I., Guertl, B., Zenz, R., Wagner, E.F., and Zatloukal, K. 1999. Functions of c-Jun in liver and heart development. *J. Cell Biol.* **145:** 1049–1061.

Ganiatsas, S., Kwee, L., Fujiwara, Y., Perkins, A., Ikeda, T., Labow, M.A., and Zon, L.I. 1998. SEK1 deficiency reveals mitogen-activated protein kinase cascade crossregulation and leads to abnormal hepatogenesis. *Proc. Natl. Acad. Sci.* **95:** 6881–6886.

Gupta, S., Campbell, D., Derijard, B., and Davis, R.J. 1995. Transcription factor ATF2 regulation by the JNK signal transduction pathway. *Science* **267:** 389–393.

Hai, T. and Curran, T. 1991. Cross-family dimerization of transcription factors Fos/Jun and ATF/CREB alters DNA binding specificity. *Proc. Natl. Acad. Sci.* **88:** 3720–3724.

Hayakawa, J., Mittal, S., Wang, Y., Korkmaz, K.S., Adamson, E., English, C., Ohmichi, M., McClelland, M., and Mercola, D. 2004. Identification of promoters bound by c-Jun/ATF2 during rapid large-scale gene activation following genotoxic stress. *Mol. Cell* **16:** 521–535.

Hilberg, F., Aguzzi, A., Howells, N., and Wagner, E.F. 1993. c-jun is essential for normal mouse development and hepatogenesis. *Nature* **365:** 179–181.

Hui, L., Bakiri, L., Mairhorfer, A., Schweifer, N., Haslinger, C., Kenner, L., Komnenovic, V., Scheuch, H., Beug, H., and Wagner, E.F. 2007. p38α suppresses normal and cancer cell proliferation by antagonizing the JNK–c-Jun pathway. *Nat. Genet.* **39:** 741–749.

Ivashkiv, L.B., Liou, H.C., Kara, C.J., Lamph, W.W., Verma, I.M., and Glimcher, L.H. 1990. mXBP/CRE-BP2 and c-Jun form a complex which binds to the cyclic AMP, but not to the 12-O-tetradecanoylphorbol-13-acetate, response element. *Mol. Cell. Biol.* **10:** 1609–1621.

Johnson, R.S., van Lingen, B., Papaioannou, V.E., and Spiegelman, B.M. 1993. A null mutation at the c-jun locus causes embryonic lethality and retarded cell growth in culture. *Genes & Dev.* **7:** 1309–1317.

Kyriakis, J.M., Banerjee, P., Nikolakaki, E., Dai, T., Rubie, E.A., Ahmad, M.F., Avruch, J., and Woodgett, J.R. 1994. The stress-activated protein kinase subfamily of c-Jun kinases. *Nature* **369:** 156–160.

Lin, A., Minden, A., Martinetto, H., Claret, F.X., Lange-Carter, C., Mercurio, F., Johnson, G.L., and Karin, M. 1995. Identification of a dual specificity kinase that activates the Jun kinases and p38–Mpk2. *Science* **268:** 286–290.

Livingstone, C., Patel, G., and Jones, N. 1995. ATF-2 contains a phosphorylation-dependent transcriptional activation domain. *EMBO J.* **14:** 1785–1797.

Maekawa, T., Bernier, F., Sato, M., Nomura, S., Singh, M., Inoue, Y., Tokunaga, T., Imai, H., Yokoyama, M., Reimold, A., et al. 1999. Mouse ATF-2 null mutants display features of a severe type of meconium aspiration syndrome. *J. Biol. Chem.* **274:** 17813–17819.

Martin-Blanco, E., Gampel, A., Ring, J., Virdee, K., Kirov, N., Tolkovsky, A.M., and Martinez-Arias, A. 1998. *puckered* encodes a phosphatase that mediates a feedback loop regulating JNK activity during dorsal closure in *Drosophila*. *Genes & Dev.* **12:** 557–570.

Nishina, H., Vaz, C., Billia, P., Nghiem, M., Sasaki, T., De la Pompa, J.L., Furlonger, K., Paige, C., Hui, C., Fischer, K.D., et al. 1999. Defective liver formation and liver cell apoptosis in mice lacking the stress signaling kinase SEK1/MKK4. *Development* **126:** 505–516.

Ouwens, D.M., de Ruiter, N.D., van der Zon, G.C., Carter, A.P., Schouten, J., van der Burgt, C., Kooistra, K., Bos, J.L., Maassen, J.A., and van Dam, H. 2002. Growth factors can activate ATF2 via a two-step mechanism: Phosphorylation of Thr71 through the Ras–MEK–ERK pathway and of Thr69 through RalGDS–Src–p38. *EMBO J.* **21:** 3782–3793.

Paumelle, R., Tulasne, D., Leroy, C., Coll, J., Vandenbunder, B., and Fafeur, V. 2000. Sequential activation of ERK and repression of JNK by scatter factor/hepatocyte growth factor in madin–darby canine kidney epithelial cells. *Mol. Biol. Cell* **11:** 3751–3763.

Porras, A., Zuluaga, S., Black, E., Valladares, A., Alvarez, A.M., Ambrosino, C., Benito, M., and Nebreda, A.R. 2004. P38 α mitogen-activated protein kinase sensitizes cells to apoptosis induced by different stimuli. *Mol. Biol. Cell* **15:** 922–933.

Pulverer, B.J., Kyriakis, J.M., Avruch, J., Nikolakaki, E., and Woodgett, J.R. 1991. Phosphorylation of c-jun mediated by MAP kinases. *Nature* **353:** 670–674.

Raingeaud, J., Gupta, S., Rogers, J.S., Dickens, M., Han, J., Ulevitch, R.J., and Davis, R.J. 1995. Pro-inflammatory cytokines and environmental stress cause p38 mitogen-activated protein kinase activation by dual phosphorylation on tyrosine and threonine. *J. Biol. Chem.* **270:** 7420–7426.

Reimold, A.M., Grusby, M.J., Kosaras, B., Fries, J.W., Mori, R., Maniwa, S., Clauss, I.M., Collins, T., Sidman, R.L., Glimcher, M.J., et al. 1996. Chondrodysplasia and neurological abnormalities in ATF-2-deficient mice. *Nature* **379:** 262–

265.
Reimold, A.M., Kim, J., Finberg, R., and Glimcher, L.H. 2001. Decreased immediate inflammatory gene induction in activating transcription factor-2 mutant mice. *Int. Immunol.* **13:** 241–248.
Rudolph, D., Yeh, W.C., Wakeham, A., Rudolph, B., Nallainathan, D., Potter, J., Elia, A.J., and Mak, T.W. 2000. Severe liver degeneration and lack of NF-κB activation in NEMO/IKKγ-deficient mice. *Genes & Dev.* **14:** 854–862.
Sanchez, I., Hughes, R.T., Mayer, B.J., Yee, K., Woodgett, J.R., Avruch, J., Kyriakis, J.M., and Zon, L.I. 1994. Role of SAPK/ERK kinase-1 in the stress-activated pathway regulating transcription factor c-Jun. *Nature* **372:** 794–798.
Smeal, T., Binetruy, B., Mercola, D.A., Birrer, M., and Karin, M. 1991. Oncogenic and transcriptional cooperation with Ha-Ras requires phosphorylation of c-Jun on serines 63 and 73. *Nature* **354:** 494–496.
Socolovsky, M., Fallon, A.E., Wang, S., Brugnara, C., and Lodish, H.F. 1999. Fetal anemia and apoptosis of red cell progenitors in Stat5a$^{-/-}$5b$^{-/-}$ mice: A direct role for Stat5 in Bcl-X(L) induction. *Cell* **98:** 181–191.
Somervaille, T.C., Linch, D.C., and Khwaja, A. 2003. Different levels of p38 MAP kinase activity mediate distinct biological effects in primary human erythroid progenitors. *Br. J. Haematol.* **120:** 876–886.
Tamura, K., Sudo, T., Senftleben, U., Dadak, A.M., Johnson, R., and Karin, M. 2000. Requirement for p38α in erythropoietin expression: A role for stress kinases in erythropoiesis. *Cell* **102:** 221–231.
van Dam, H., Wilhelm, D., Herr, I., Steffen, A., Herrlich, P., and Angel, P. 1995. ATF-2 is preferentially activated by stress-activated protein kinases to mediate c-jun induction in response to genotoxic agents. *EMBO J.* **14:** 1798–1811.
Ventura, J.J., Tenbaum, S., Perdiguero, E., Huth, M., Guerra, C., Barbacid, M., Pasparakis, M., and Nebreda, A.R. 2007. p38α MAP kinase is essential in lung stem and progenitor cell proliferation and differentiation. *Nat. Genet.* **39:** 750–758.
Vinson, C., Myakishev, M., Acharya, A., Mir, A.A., Moll, J.R., and Bonovich, M. 2002. Classification of human B-ZIP proteins based on dimerization properties. *Mol. Cell. Biol.* **22:** 6321–6335.
Wilkinson, M.G., Samuels, M., Takeda, T., Toone, W.M., Shieh, J.C., Toda, T., Millar, J.B., and Jones, N. 1996. The Atf1 transcription factor is a target for the Sty1 stress-activated MAP kinase pathway in fission yeast. *Genes & Dev.* **10:** 2289–2301.
Wu, J.J. and Bennett, A.M. 2005. Essential role for mitogen-activated protein (MAP) kinase phosphatase-1 in stress-responsive MAP kinase and cell survival signaling. *J. Biol. Chem.* **280:** 16461–16466.